Chaos, Solitons and Fractals 123 (2019) 43–51

Contents lists available at ScienceDirect

Chaos, Solitons and Fractals

Nonlinear Science, and Nonequilibrium and Complex Phenomena

journal homepage: www.elsevier.com/locate/chaos

Frontiers

Dynamical behaviour of fractional order tumor model with Caputo and conformable fractional derivative☆

Ercan Balcı[a,*], İlhan Öztürk[a], Senol Kartal[b]

[a] Department of Mathematics, Erciyes University, Kayseri 38039, Turkey
[b] Department of Science and Mathematics Education, Nevsehir Haci Bektas Veli University, Nevsehir 50300, Turkey

ARTICLE INFO

Article history:
Received 27 January 2019
Revised 20 March 2019
Accepted 28 March 2019
Available online 2 April 2019

Keywords:
Tumor-immune interaction
Fractional order
Piecewise-constant arguments
Neimark-Sacker bifurcation
Conformable fractional derivative

ABSTRACT

In this paper, tumor-immune system interaction has been considered by two fractional order models. The first and the second model consist of system of fractional order differential equations with Caputo and conformable fractional derivative respectively. First of all, the stability of the equilibrium points of the first model is studied. Then, a discretization process is applied to obtain a discrete version of the second model where conformable fractional derivative is taken into account. In discrete model, we analyze the stability of the equilibrium points and prove the existence of Neimark-Sacker bifurcation depending on the parameter σ. Moreover, the dynamical behaviours of the models are compared with each other and we observe that the discrete version of conformable fractional order model exhibits chaotic behavior. Finally, numerical simulations are also presented to illustrate the analytical results.

1. Introduction

Research on fractional calculus has gained much interest over the past decades and furthermore, fractional order differential equations has been well applied to many research field such as physics [1,2], chemistry [3], medicine [5], finance [4] and engineering [6]. These equations are also widely used to model biological phenomenon and there are successful applications in this field. It is also demonstrated that biological models constructed by fractional order differential equations exhibit more realistic results comparing with integer order counterpart [7–9]. This is for the reason that fractional order derivatives involve memory and which is quite favorable to work on biological processes.

Trying to generalize notion of differentiation to arbitrary order brings out several approaches. The most knowns are Riemann-Liouville, Caputo and Grünwald-Letnikov definitions [10]. In addition to these definitions, a new definition called "conformable fractional derivative" has been introduced by Khalil et al. in 2014 [13]. According to this definition, the left fractional derivative starting from a of the function f: $[a, \infty) \to \infty$ of order $0 < \alpha \leq 1$ has its own limit-based definition as follows:

$$(T_\alpha^a f)(t) = \lim_{\epsilon \to 0} \frac{f(t + \epsilon(t-a)^{1-\alpha}) - f(t)}{\epsilon}$$

provided the limit exist. The right fractional derivative of order $0 < \alpha \leq 1$ terminating at b of f is defined by

$$({}_\alpha^b T f)(t) = -\lim_{\epsilon \to 0} \frac{f(t + \epsilon(b-t)^{1-\alpha}) - f(t)}{\epsilon}.$$

Note also that if f is differentiable in usual sense, we have the following equalities:

$$(T_\alpha^a f)(t) = (t-a)^{1-\alpha} f'(t), \qquad ({}_\alpha^b T f)(t) = (t-b)^{1-\alpha} f'(t). \quad (1)$$

Unlike classical fractional derivative definitions, conformable fractional derivative share some basic properties with integer order derivative. In [14], Abdeljawad introduced conformable versions of exponential functions, Gronwall's inequality, integration by parts, Taylor series expansion and Laplace transforms. Moreover, biological and physical applications of conformable fractional derivative can be found in [15–19].

Together with these definitions, there are numerous approaches being studied by applied mathematicians. Researchers trying to find the most efficient approach while constructing or adjusting their models. Meanwhile, some numerical methods such as Adomian decomposition [20], Adams-type predictor-corrector [21] and homotopy perturbation method [22] are also developed to solve fractional differential equations [23]. In addition to the these numerical methods, several papers have used piecewise constant approximations to discretize fractional order differential equations

☆ This work was supported by Research Fund of the Erciyes University. Project Number: FDK-2018-8119.

* Corresponding author.
E-mail addresses: ercanbalci@erciyes.edu.tr (E. Balcı), ozturki@erciyes.edu.tr (İ. Öztürk), senol.kartal@nevsehir.edu.tr (S. Kartal).

https://doi.org/10.1016/j.chaos.2019.03.032
0960-0779/

[27–29]. In [17], Kartal and Gurcan considered the conformable fractional logistic equation with piecewise constant arguments with adopting the method presented by Gopalsamy in [30].

The tumor-immune interaction model studied in this paper originated from the following model presented by Kuznetsov et al. [24]:

$$\begin{cases} \frac{dE}{dt} = s + F(E,T) - mET - dE, \\ \frac{dT}{dt} = aT(1-bT) - nET, \end{cases} \tag{2}$$

where $F(E,T) = \frac{pET}{g+T}$. In study [25], Galach suppose that $F(E,T) = \theta ET$ and thus model (2) takes the form

$$\begin{cases} \frac{dE}{dt} = s + \alpha_1 ET - dE, \\ \frac{dT}{dt} = aT(1-bT) - nET, \end{cases} \tag{3}$$

where $\alpha_1 = \theta - m$. Then, the dimensionless form of the model (3) can be obtained as

$$\begin{cases} \frac{dx}{dt} = \sigma + wxy - \delta x, \\ \frac{dy}{dt} = \gamma y(1-\beta y) - xy, \end{cases} \tag{4}$$

where x and y denote the dimensionless density of ECs and TCs respectively, $x = E/E_0$, $y = T/T_0$, ,$\gamma = \frac{a}{nT_0}$ $\beta = bT_0$, $\delta = \frac{d}{nT_0}$, $\sigma = \frac{s}{nE_0T_0}$, $\omega = \alpha_1/n$, E_0 and T_0 are the initial conditions.

In the study [26], the fractional order form of the model (4) is considered with the Caputo sense as follows:

$$\begin{cases} D^\alpha x(t) = \sigma + \omega xy - \delta x, \\ D^\alpha y(t) = \gamma y(1-\beta y) - xy, \end{cases} \tag{5}$$

with initial conditions $x(0) = x_0 \geq 0$ and $y(0) = y_0 \geq 0$. Thus, conformable fractional order version of the model (4) is given as follows:

$$\begin{cases} T_\alpha E(t) = \sigma + \omega ET - \delta E, \\ T_\alpha T(t) = \gamma T(1-\beta T) - ET \end{cases} \tag{6}$$

where we take $\alpha \in (0, 1]$ as conformable fractional order.

The aim of this study is to investigate the dynamical behaviour of model (5) and model (6) and to compare the obtained results.

2. Dynamical behaviour of fractional order tumor model

Here, we adopt fractional order model (5) with Caputo fractional derivative which is defined by

$$D_a^\alpha f(t) = \int_a^t \frac{f^n(x)}{(t-x)^{\alpha-n+1}} dx.$$

2.1. Stability analysis

Theorem 1 *[11,12]. Consider the system*

$$D_a^\alpha f(t) = f(t, X(t)), \quad X(t_0) = X_0. \tag{7}$$

Let $J(X^*)$ denote the Jacobian matrix of the system (7) evaluated at the equilibrium point X^*.

(1) *The equilibrium point X^* is locally asymptotically stable if and only if all the eigenvalues λ_i, $i = 1, 2, \ldots, n$ of $J(X^*)$ satisfy $|arg(\lambda_i)| > \frac{\alpha\pi}{2}$,*
(2) *The equilibrium point X^* is stable if all the eigenvalues λ_i, $i = 1, 2, \ldots, n$ of $J(X^*)$ satisfy $|arg(\lambda_i)| \geq \frac{\alpha\pi}{2}$ and eigenvalues with $|arg(\lambda_i)| = \frac{\alpha\pi}{2}$ have the same geometric and algebraic multiplicity, and*
(3) *The equilibrium point X^* is unstable if and only if there exist eigenvalues λ_i for some $i = 1, 2, \ldots, n$ of $J(X^*)$ satisfy $|arg(\lambda_i)| < \frac{\alpha\pi}{2}$.*

An equilibrium point of model (5) is obtained by solving the following system:

$$\begin{cases} D^\alpha x(t) = 0, \\ D^\alpha y(t) = 0. \end{cases}$$

That is

$$\begin{cases} \sigma + \omega xy - \delta x = 0, \\ \gamma y(1-\beta y) - xy = 0. \end{cases}$$

Hence, we have two equilibrium points:

i. The tumor-free equilibrium point $E_0 = (\frac{\sigma}{\delta}, 0)$,
ii. The coexistence equilibrium point
$E_1 = (\overline{E}, \overline{T}) = (\frac{\gamma(-\beta\delta+\omega)+\sqrt{\Delta}}{2\omega}, \frac{\gamma(\beta\delta+\omega)-\sqrt{\Delta}}{2\gamma\beta\omega})$

where $\Delta = 4\gamma\beta\sigma\omega + \gamma^2(\beta\delta - \omega)^2$. Under the condition $\sigma < \gamma\delta$, the coexistence equilibrium point is always positive.

Theorem 2. *For the equilibrium point $E_0 = (\frac{\sigma}{\delta}, 0)$ of model (5), the following results holds true;*

i. If $\sigma > \gamma\delta$, then E_0 is locally asymptotically stable,
ii. If $\sigma < \gamma\delta$, then E_0 is unstable and is a saddle point.

Proof. The Jacobian matrix of the model (5) evaluated at equilibrium point E_0 is given by

$$J(E_0) = \begin{pmatrix} -\delta & \frac{\sigma\omega}{\delta} \\ 0 & \gamma - \frac{\sigma}{\delta} \end{pmatrix}.$$

Hence the eigenvalues of $J(E_0)$ are $\lambda_1 = -\delta$ and $\lambda_2 = \gamma - \frac{\sigma}{\delta}$. Since $\lambda_1 < 0$, we have $arg(\lambda_1) = \pi$ which satisfies $|arg(\lambda_1)| > \frac{\alpha\pi}{2}$. If $\sigma > \gamma\delta$, then $\lambda_2 < 0$ and $arg(\lambda_2) = \pi$ which results in $|arg(\lambda_2)| > \frac{\alpha\pi}{2}$. According to Theorem 1, equilibrium point E_0 is locally asymptotically stable if $\sigma > \gamma\delta$. If $\sigma < \gamma\delta$, then $\lambda_2 > 0$. Hence $arg(\lambda_2) = 0$, which always satisfies $|arg(\lambda_2)| < \frac{\alpha\pi}{2}$. By Theorem 1, the equilibrium point E_0 is a saddle point so unstable. □

Theorem 3. *Consider the coexistence equilibrium point E_1 of the model (5). Under the positivity condition $\sigma < \gamma\delta$, E_1 is locally asymptotically stable. Moreover, if $\sigma = \frac{\beta\gamma^2\delta(\beta(\gamma+\delta)-\omega)}{(-\beta\gamma+\omega)^2}$, E_1 is asymptotically stable under the condition $\gamma < \frac{\omega^2}{\beta^2\delta+\delta\omega}$.*

Proof. The Jacobian matrix of the model (5) evaluated at equilibrium point E_1 is given by

$$J(E_1) = \begin{pmatrix} -\frac{\beta\gamma\delta+\sqrt{\Delta}-\gamma\omega}{2\beta\gamma} & \frac{1}{2}(-\beta\gamma\delta+\sqrt{\Delta}+\gamma\omega) \\ \frac{\sqrt{\Delta}-\gamma(\beta\delta+\omega)}{2\beta\gamma\omega} & \frac{\sqrt{\Delta}-\gamma(\beta\delta+\omega)}{2\omega} \end{pmatrix}.$$

Then, under the positivity condition $\sigma < \gamma\delta$ of the coexistence equilibrium point, the determinant and the trace of $J(E_1)$ are

$$\begin{aligned} det(J(E_1)) &= \frac{\sqrt{\delta}(\beta\gamma\delta - \sqrt{\Delta} + \gamma\omega)}{2\beta\gamma\omega} > 0 \\ tr(J(E_1)) &= \frac{1}{2}\left(-\frac{\beta\gamma\delta+\sqrt{\Delta}-\gamma\omega}{\beta\gamma} + \frac{\sqrt{\Delta}-\gamma(\beta\delta+\omega)}{\omega}\right) \leq 0. \end{aligned}$$

Thus, the eigenvalues of $J(E_2)$ are written as

$$\begin{aligned} \lambda_1 &= \frac{1}{2}\left(tr(J(E_1)) + \sqrt{tr^2(J(E_1)) - 4det(J(E_1))}\right) \\ \lambda_2 &= \frac{1}{2}\left(tr(J(E_1)) - \sqrt{tr^2(J(E_1)) - 4det(J(E_1))}\right) \end{aligned}$$

If $tr^2(J(E_1)) - 4det(J(E_1)) > 0$, then the eigenvalues becomes negative real numbers; if $tr^2(J(E_1)) - 4det(J(E_1)) < 0$, then we obtain a pair of complex conjugate eigenvalues λ_1 and $\lambda_2 = \overline{\lambda_1}$. Since $tr(J(E_1)) < 0$, we have $Re(\lambda_1) = Re(\lambda_2) < 0$ and consequently we have $|arg(\lambda_{1,2})| > \frac{\alpha\pi}{2}$.

If $\sigma = \frac{\beta\gamma^2\delta(\beta(\gamma+\delta)-\omega)}{(-\beta\gamma+\omega)^2}$, then $tr(J(E_1)) = 0$. So, we obtain a pair of complex conjugate eigenvalues λ_1 and $\lambda_2 = \overline{\lambda_1}$. Since $Re(\lambda_1) = Re(\lambda_2) = tr(J(E_1)) = 0$, we have $arg(\lambda_1) = \frac{\pi}{2}$ and $arg(\lambda_2) = -\frac{\pi}{2}$ leading to $|arg(\lambda_{1,2})| > \frac{\alpha\pi}{2}$. □

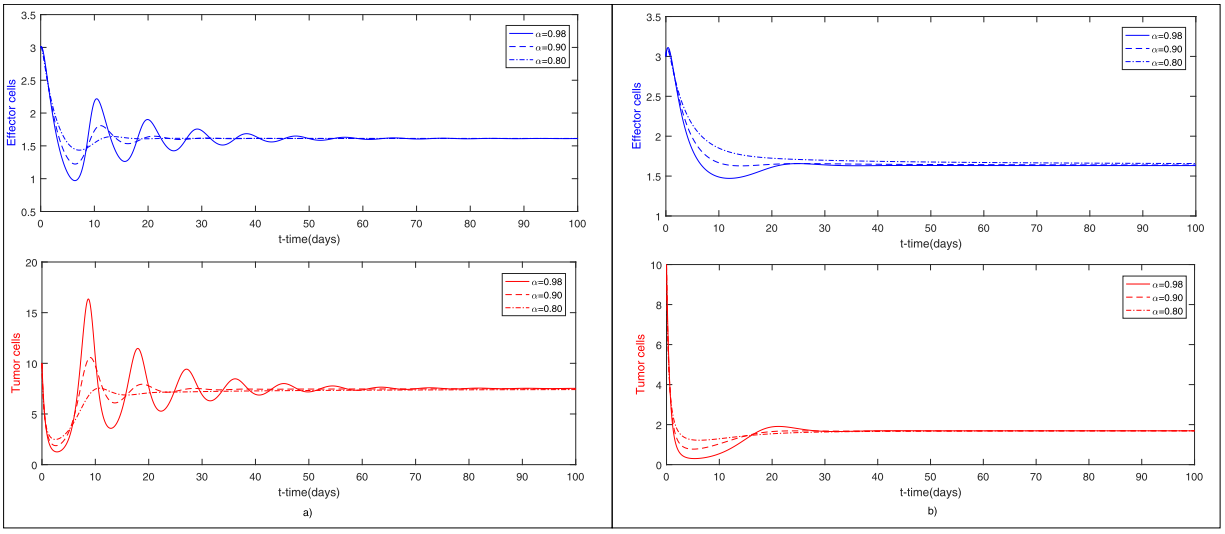

Fig. 1. Stable dynamical behaviour of the model (5) for the parameter values given in Table 1 with $\sigma = 0.1181$ in (a) and $\sigma = 0.5$ in (b) with initial condition $(E, T) = (3, 10)$ where blue and red curves represent population density of ECs and TCs respectively. (For interpretation of the references to colour in this figure legend, the reader is referred to the web version of this article.)

2.2. Numerical simulations

In this section, the predictor-corrector method is used for numerical simulations of the model (5). This method introduced in [36,37] which is a combination of some product integration rules, known as fractional Adams-Bashforthm-Moulton methods [38].

To analyze the effects of the model parameters on its dynamics, it is easier to make qualitative analysis on the dimensionless form of the model (3). That is why we obtained non-dimensionalized model on which qualitative analysis is performed.

In Fig. 1, we get asymptotically stable coexistence equilibrium points for different values of σ. In Fig. 1a for smaller values of σ, we observed an oscillatory behaviour for both ECs and TCs. According to Theorem 1, fractional derivatives enlarges the regions of stability. Here, we also observed that smaller fractional order derivatives damps the oscillation behavior and for smaller fractional derivatives, both ECs and TCs approaches quicker to the equilibrium point. In Fig. 1b for $\sigma = 0.5$, ECs are more successful but insufficient in eradicating the TCs and oscillatory behaviour disappears comparing with Fig. 1a. Both situations corresponds to the dormant tumor state [24,25].

3. Dynamical behavior of conformable fractional order tumor model

3.1. Discretizations process

In this section, we will discretize the model (6) by using piecewise constant approximation [17]. Consider the conformable fractional order model (6) as

$$\begin{cases} T_\alpha E(t) = \sigma + \omega E(t)T([\frac{t}{h}]h) - \delta E(t), \\ T_\alpha T(t) = \gamma T(t)(1-\beta T(t)) - E([\frac{t}{h}]h)T(t), \end{cases} \tag{8}$$

with $E(0) = E_0$ and $T(0) = T_0$, where $[t]$ denotes the integer part of $t \in [0, \infty)$ and $h > 0$ is discretization parameter.

Appliying the property (1) of conformable fractional derivative to the first equation of the system (8) for $t \in [nh, (n+1)h)$ gives

$$(t-nh)^{1-\alpha}\frac{dE(t)}{dt} = \sigma + \omega E(t)T(nh) - \delta E(t).$$

By simplifying this equation, we get

$$E'(t) + E(t)\left[\frac{\delta - \omega T(nh)}{(t-nh)^{1-\alpha}}\right] = \frac{\sigma}{(t-nh)^{1-\alpha}}.$$

Clearly, this is a first-order linear ordinary differential equation. Solving this equation with respect to $t \in [nh, t)$, we obtain

$$E(t) = \frac{(\delta - \omega T(nh))E(nh) + \sigma\left(e^{(\delta-\omega T(nh))\frac{(t-nh)^\alpha}{\alpha}} - 1\right)}{e^{(\delta-\omega T(nh))\frac{(t-nh)^\alpha}{\alpha}}(\delta - \omega T(nh))}$$

and by taking $t \to (n+1)h$, we get the following difference equation

$$E((n+1)h) = \frac{\sigma + [(\delta - \omega T(nh))E(nh) - \sigma]e^{(\omega T(nh)-\delta)\frac{h^\alpha}{\alpha}}}{\delta - \omega T(nh)}.$$

Finally, adjusting difference equation notation and replacing $E(nh)$ and $T(nh)$ by $E(n)$ and $T(n)$ yields

$$E(n+1) = \frac{\sigma + [(\delta - \omega T(n))E(n) - \sigma]e^{(\omega T(n)-\delta)\frac{h^\alpha}{\alpha}}}{\delta - \omega T(n)}.$$

In a similar fashion, discretizing the second equation of the system (8)

$$T_\alpha T(t) = \gamma T(t)(1-\beta T(t)) - E\left(\left[\frac{t}{h}\right]h\right)T(t)$$

leads to the following difference equation

$$T(n+1) = \frac{T(n)(\gamma - E(n))}{(\gamma - E(n) - \gamma\beta T(n))e^{(E(n)-\gamma)\frac{h^\alpha}{\alpha}} + \gamma\beta T(n)}.$$

Therefore, we get the two-dimensional discrete system

$$\begin{cases} E(n+1) = \frac{\sigma + [(\delta-\omega T(n))E(n) - \sigma]e^{(\omega T(n)-\delta)\frac{h^\alpha}{\alpha}}}{\delta - \omega T(n)} \\ T(n+1) = \frac{T(n)(\gamma - E(n))}{(\gamma - E(n) - \gamma\beta T(n))e^{(E(n)-\gamma)\frac{h^\alpha}{\alpha}} + \gamma\beta T(n)} \end{cases}. \tag{9}$$

3.2. Stability analysis

Now, we analyze local asymptotic stability of the system (9). We note that system (9) and system (5) have the same equilibrium points that is E_0, E_1.

We linearize the system (9) about the equilibrium point E_0. The associated Jacobian matrix has eigenvalues $\lambda_1 = e^{-\frac{h^\alpha \delta}{\alpha}}$ and

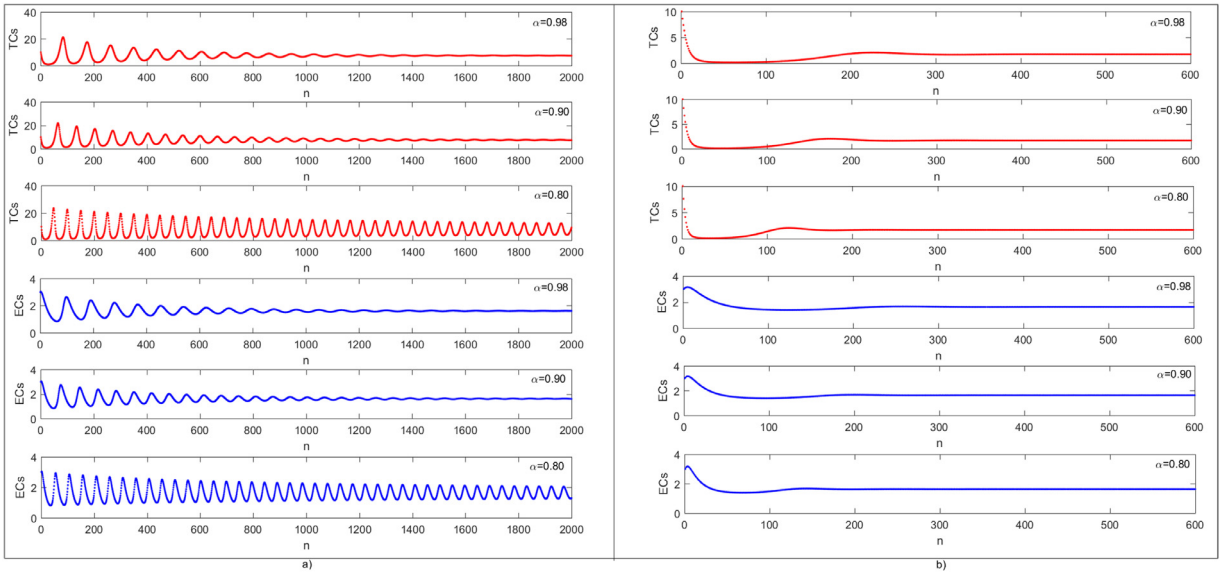

Fig. 2. Stable dynamical behaviours of the model (9) for the parameter values given in Table 1 with $\sigma = 0.1181$ in (a), $\sigma = 0.5$ in (b) and initial condition $(E, T) = (3, 10)$ where blue and red curves represents population density of ECs and TCs respectively. (For interpretation of the references to colour in this figure legend, the reader is referred to the web version of this article.)

$\lambda_2 = e^{-\frac{h^\alpha(\sigma-\gamma\delta)}{\alpha\delta}}$. It is easy to prove that E_0 is locally asymptotically stable if $\gamma\delta < \sigma$, and unstable if $\gamma\delta > \sigma$.

The equilibrium point E_1 has nonnegative coordinates if the condition $\sigma < \delta\gamma$ is satisfied. Now, the Jacobian matrix obtained by linearizing the system (9) about the equilibrium point $E_1 = (\overline{E}, \overline{T})$ is given by

$$A_{(\overline{E},\overline{T})} = \begin{pmatrix} a_{11} & a_{12} \\ a_{21} & a_{22} \end{pmatrix} = \begin{pmatrix} e^{-\frac{h^\alpha c}{2\alpha\beta\gamma}} & \frac{4\beta^2\gamma^2\sigma\omega(1-e^{-\frac{h^\alpha c}{2\alpha\beta\gamma}})}{c^2} \\ \frac{-1+e^{-\frac{h^\alpha d}{2\alpha\omega}}}{\beta\gamma} & e^{-\frac{h^\alpha d}{2\alpha\omega}} \end{pmatrix}$$

where

$$c = \beta\gamma\delta + \sqrt{\Delta} - \gamma\omega \quad \text{and} \quad d = \beta\gamma\delta - \sqrt{\Delta} + \gamma\omega.$$

The corresponding characteristic polynomial is

$$\lambda^2 + p_1\lambda + p_0$$

where

$$p_0 = e^{-\frac{h^\alpha c}{2\alpha\beta\gamma}} e^{-\frac{h^\alpha d}{2\alpha\omega}} + \frac{4\left(1-e^{-\frac{h^\alpha c}{2\alpha\beta\gamma}}\right)\left(1-e^{-\frac{h^\alpha d}{2\alpha\omega}}\right)\beta\gamma\sigma\omega}{c^2},$$
$$p_1 = -\left(e^{-\frac{h^\alpha c}{2\alpha\beta\gamma}} + e^{-\frac{h^\alpha d}{2\alpha\omega}}\right).$$

Theorem 4. *Assume that $\sigma < \delta\gamma$. The coexistence equilibrium point $(\overline{E}, \overline{T})$ is locally asymptotically stable if and only if*

$$\sigma > \overline{\sigma} = \frac{\left(e^{\frac{h^\alpha(-\sqrt{\Delta}-\gamma(\beta\delta-\omega))}{2\alpha\beta\gamma}} - e^{\frac{h^\alpha(\beta\gamma\delta-\sqrt{\Delta}+\gamma\omega)}{2\alpha\omega}}\right)c^2}{4\left(-1+e^{\frac{h^\alpha(-\sqrt{\Delta}-\gamma(\beta\delta-\omega))}{2\alpha\beta\gamma}}\right)\left(-1+e^{\frac{h^\alpha(\beta\gamma\delta-\sqrt{\Delta}+\gamma\omega)}{2\alpha\omega}}\right)\beta\gamma\omega}. \tag{10}$$

Proof. To check asymptotically stability of E_1, we use the following Jury conditions [31]:

$$i)\ 1 + p_1 + p_0 > 0, \qquad ii)\ 1 - p_1 + p_0 > 0, \qquad iii)\ 1 - p_0 > 0.$$

Under assumption $\sigma < \delta\gamma$, we always have $c,\ d > 0$. These two inequality assures that

$$0 < e^{-\frac{h^\alpha c}{2\alpha\beta\gamma}}, e^{-\frac{h^\alpha d}{2\alpha\omega}} < 1 \tag{11}$$

and consequently we have

$$1 + p_1 + p_0 = \left(1 - e^{-\frac{h^\alpha c}{2\alpha\beta\gamma}}\right)\left(1 - e^{-\frac{h^\alpha d}{2\alpha\omega}}\right) + \frac{4\left(1 - e^{-\frac{h^\alpha c}{2\alpha\beta\omega}}\right)\left(1 - e^{-\frac{h^\alpha d}{2\alpha\omega}}\right)\beta\gamma\sigma\omega}{c^2} > 0,$$

$$1 - p_1 + p_0 = \left(1 + e^{-\frac{h^\alpha c}{2\alpha\beta\gamma}}\right)\left(1 + e^{-\frac{h^\alpha d}{2\alpha\omega}}\right) + \frac{4\left(1 - e^{-\frac{h^\alpha c}{2\alpha\beta\omega}}\right)\left(1 - e^{-\frac{h^\alpha d}{2\alpha\omega}}\right)\beta\gamma\sigma\omega}{c^2} > 0.$$

In addition, under the condition (10), we have

$$p_0 = e^{-\frac{h^\alpha c}{2\alpha\beta\gamma}} e^{-\frac{h^\alpha d}{2\alpha\omega}} + \frac{4\left(1-e^{-\frac{h^\alpha c}{2\alpha\beta\gamma}}\right)\left(1-e^{-\frac{h^\alpha d}{2\alpha\omega}}\right)\beta\gamma\sigma\omega}{c^2} < 1, \tag{12}$$

essentially $1 - p_0 > 0$ and the proof is completed.

Fig. 2 shows asymptotically stable coexistence equilibrium points for different values of σ similarly to Fig. 1. In Fig. 2a for smaller values of σ, we observed more oscillatory behaviour for both ECs and TCs comparing with Fig. 1a. This is for the reason that, $\sigma = 0.1181$ is very close to the critical value $\overline{\sigma} = 0.075445$ in Theorem 4 which will be the critical threshold for Neimark-Sacker bifurcation as we will see in next section. In Fig. 1b for $\sigma = 0.5$, the system loses its oscillatory behavior and the tumor cells extinct for a while, then approaches to the coexistence equilibrium point. This situation corresponds to the state of a "returning tumor"[35]. Moreover, in Fig. 1b we observe that for a smaller fractional derivatives, both ECs and TCs approaches quicker to the equilibrium point.

3.3. Neimark-Sacker bifurcation analysis

In this section, we analyze the Neimark-Sacker bifurcation of the system (9) at the equilibrium point E_1.

First of all, we convert the equilibrium point $E_1 = (\overline{E}, \overline{T})$ of the system (9) into the origin by change of variables $x_1 = E - \overline{E}$ and $x_2 = N - \overline{N}$. Thus, the system (9) turns into

$$\begin{pmatrix} x_1 \\ x_2 \end{pmatrix} \to A(\sigma)\begin{pmatrix} x_1 \\ x_2 \end{pmatrix} + \begin{pmatrix} F_1(x_1, x_2, \sigma) \\ F_2(x_1, x_2, \sigma) \end{pmatrix} \tag{13}$$

where

$$A(\sigma) = A_{(\overline{E},\overline{T})}$$

and

$$F_1(x_1,x_2,\sigma)=\frac{h^\alpha a_{11}\omega}{\alpha}x_1x_2+\frac{h^{2\alpha}a_{11}\omega^2}{2\alpha^2}x_1x_2^2 -\frac{8a_{11}\beta^2\gamma^2\sigma\omega^2((2-2/a_{11})\alpha\beta\gamma+h^\alpha c}{2\alpha c^3}x_2^2-\frac{12a_{11}\beta^2\gamma^2\sigma\omega^3}{6\alpha^2c^4} \times((8-8/a_{11})\alpha^2\beta^2\gamma^2+4h^\alpha\alpha\beta\gamma c+h^{2\alpha}c^2)x_2^3+O(|X|^4),$$

$$\begin{aligned}F_2(x_1,x_2,\sigma)=&\frac{2a_{22}((-2+2a_{22})\alpha\omega+h^\alpha d)}{2\alpha\beta\gamma d}x_1^2+\frac{4(-a_{22}+a_{22}^2)\beta\gamma\omega}{2d}x_2^2\\&+\frac{a_{22}((-4+4a_{22})\alpha\omega+h^\alpha d)}{\alpha d}x_1x_2\\&+\frac{3a_{22}}{6\alpha^2\beta\gamma d^2}(-8a_{22}^2(-1+1/a_{22})\alpha^2\omega^2\\&+4(-1+2a_{22})h^\alpha\alpha\omega d+h^{2\alpha}d^2)x_1^3+\frac{a_{22}}{2\alpha^2d^2}(8\alpha^2\omega^2\\&+24a_{22}^2\alpha^2\omega^2-8h^\alpha\alpha\omega d+h^{2\alpha}d^2\\&-16a_{22}\alpha\omega(2\alpha\omega-h^\alpha d))x_1^2x_2+\frac{4a_{22}^3\beta\gamma\omega}{2\alpha d^2}(6\alpha\omega\\&+1/a_{22}^2(4\alpha\omega-h^\alpha d)-(2/a_{22})(5\alpha\omega-h^\alpha d))x_1x_2^2\\&+\frac{24a_{22}^3(-1+1/a_{22})^2\beta^2\gamma^2\omega^2}{6d^2}x_2^3+O(|X|^4).\end{aligned}$$

For $\sigma=\overline{\sigma}$, the eigenvalues of $A(\overline{\sigma})$ are

$$\lambda_{1,2}(\overline{\sigma})=\frac{-p_1(\overline{\sigma})\pm i\sqrt{p_1(\overline{\sigma})^2-4p_0(\overline{\sigma})}}{2}$$

where

$$p_1(\overline{\sigma})=-e^{-\frac{h^\alpha(\beta\gamma\delta+\sqrt{4\gamma\beta\overline{\sigma}\omega+\gamma^2(\beta\delta-\omega)^2}-\gamma\omega)}{2\alpha\beta\gamma}}-e^{\frac{h^\alpha(\sqrt{4\gamma\beta\overline{\sigma}\omega+\gamma^2(\beta\delta-\omega)^2}-\gamma(\beta\delta+\omega))}{2\alpha\omega}}$$

and

$$p_0(\overline{\sigma})=1.$$

Moreover, we obtain $|\lambda_{1,2}(\overline{\sigma})|=1$. So, the eigenvalues of $A(\overline{\sigma})$ are complex conjugates with modulus 1 as required. In addition, $p_1(\overline{\sigma})\neq 0,1$ and we can conclude that $\lambda_{1,2}^k(\overline{\sigma})\neq 1$ for $k=1,2,3,4$. Hence, non-strong resonance condition is also satisfied.

The transversality condition yields to the inequality

$$\frac{d|\lambda_{1,2}(\sigma)|}{d\sigma}\Big|_{\sigma=\overline{\sigma}}=\frac{2\beta\gamma\omega\left(e^{\frac{h^\alpha(\beta\gamma\delta+\sqrt{\Delta})}{2\alpha\beta\gamma}}-e^{\frac{h^\alpha\beta}{2\beta}}\right)\left(e^{\frac{h^\alpha\sqrt{\Delta}}{2\alpha\omega}}-e^{\frac{h^\alpha\gamma(\beta\delta+\omega)}{2\alpha\omega}}\right)}{e^{\frac{h^\alpha(\beta^2\gamma^2\delta+\gamma\omega(\gamma+\delta)+\sqrt{\Delta}\omega)}{2\alpha\beta\gamma\omega}}(\beta\gamma\delta+\sqrt{\Delta}-\gamma\omega)^2}\neq 0$$

which is satisfied for positive parameters and $\sigma<\beta\gamma$.

Now, we calculate multilinear functions:

$$\begin{aligned}B_1(x,y)&=\sum_{j,k=1}^{2}\frac{\partial^2F_1(\psi,\sigma)}{\partial\psi_j\partial\psi_k}\Big|_{\psi=0}x_jy_k\\&=\frac{h^\alpha a_{11}\omega}{\alpha}(x_1y_2+x_2y_1)\\&\quad-\frac{(8a_{11}\beta^2\gamma^2\sigma\omega^2(2-2/a_{11})\alpha\beta\gamma+h^\alpha c)}{\alpha c^3}x_2y_2,\end{aligned}$$

$$\begin{aligned}B_2(x,y)&=\sum_{j,k=1}^{2}\frac{\partial^2F_2(\psi,\sigma)}{\partial\psi_j\partial\psi_k}\Big|_{\psi=0}x_jy_k\\&=\frac{2a_{22}((-2+2a_{22})\alpha\omega+h^\alpha d)}{\alpha\beta\gamma d}x_1y_1\\&\quad+\frac{4(-a_{22}+a_{22}^2)\beta\gamma\omega}{d}x_2y_2\\&\quad+\frac{a_{22}((-4+4a_{22})\alpha\omega+h^\alpha d)}{\alpha d}(x_1y_2+x_2y_1),\end{aligned}$$

$$\begin{aligned}C_1(x,y,u)&=\sum_{j,k,l=1}^{2}\frac{\partial^3F_1(\psi,\sigma)}{\partial\psi_j\partial\psi_k\partial\psi_l}\Big|_{\psi=0}x_jy_ku_l\\&=\frac{h^{2\alpha}a_{11}\omega^2}{\alpha^2}(x_2y_2u_1+x_2y_1u_2+x_1y_2u_2)\\&\quad-\frac{12a_{11}\beta^2\gamma^2\sigma\omega^3}{\alpha^2c^4}x_2y_2u_2((8-8a_{22})\alpha^2\beta^2\gamma^2\\&\quad+4h^\alpha\alpha\beta\gamma c+h^{2\alpha}c^2),\end{aligned}$$

$$\begin{aligned}C_2(x,y,u)&=\sum_{j,k,l=1}^{2}\frac{\partial^3F_2(\psi,\sigma)}{\partial\psi_j\partial\psi_k\partial\psi_l}\Big|_{\psi=0}x_jy_ku_l\\&=\frac{3a_{22}}{\alpha^2\beta\gamma d^2}(8a_{22}(-1+a_{22})\alpha^2\omega^2\\&\quad+4(-1+2a_{22})h^\alpha\alpha\omega d+h^{2\alpha}d^2)x_1y_1u_1\\&\quad+\frac{a_{22}}{\alpha^2d^2}(8\alpha^2\omega^2+24a_{22}^2\alpha^2\omega^2-8h^\alpha\alpha\omega d+h^{2\alpha}d^2\\&\quad-16a_{22}\alpha\omega(2\alpha\omega-h^\alpha d))(x_2y_1u_1+x_1y_2u_1+x_1y_1u_2)\\&\quad+\frac{4a_{22}\beta\gamma\omega}{\alpha d^2}(2(2-5a_{22}+3a_{22}^2)\alpha\omega\\&\quad+(-1+2a_{22})h^\alpha d)(x_2y_2u_1+x_2y_1u_2+x_1y_2u_2)\\&\quad+\frac{24a_{22}(-1+a_{22})^2\beta^2\gamma^2\omega^2}{d^2}x_2y_2u_2.\end{aligned}$$

Now, let $q\sim(\zeta_1+i\zeta_2,1)\in\mathbf{C}^2$ be an eigenvector of $A(\overline{\sigma})$ corresponding to $\lambda_1(\overline{\sigma})$ and let $\bar{p}\sim(\xi_1+i\xi_2,1)\in\mathbf{C}^2$ be an eigenvector of $A^T(\overline{\sigma})$ corresponding to $\lambda_2(\overline{\sigma})$. Afterwards, we normalize $\bar{p}$ with respect to q. Hence, q and the normalized vector p are computed:

$$p=\left(\frac{\xi_1+i\xi_2}{1+(\xi_1+i\xi_2)(\zeta_1-i\zeta_2)},\frac{1}{1+(\xi_1+i\xi_2)(\zeta_1-i\zeta_2)}\right),$$
$$q=(\zeta_1+i\zeta_2,1)$$

where

$$\xi_1=\frac{\left(-1+e^{\frac{h^\alpha d}{2\alpha\omega}}\right)\left(-1+e^{\frac{h^\alpha(\beta\gamma(\beta\gamma\delta-\sqrt{\Delta})+(\beta\gamma(\gamma-\delta)-\sqrt{\Delta})\omega+\gamma\omega^2}{2\alpha\beta\gamma\omega}}\right)}{2\beta\gamma\left(e^{\frac{h^\alpha d}{\alpha\omega}}-e^{\frac{h^\alpha(\beta\gamma(\beta\gamma\delta-\sqrt{\Delta})+(\beta\gamma(\gamma-\delta)-\sqrt{\Delta})\omega+\gamma\omega^2}{2\alpha\beta\gamma\omega}}\right)}$$

$$\xi_2=\frac{\left(-1+e^{\frac{h^\alpha d}{2\alpha\omega}}\right)e^{\frac{h^\alpha d}{2\alpha\omega}}}{2\beta\gamma\left(e^{\frac{h^\alpha d}{\alpha\omega}}-e^{\frac{h^\alpha(\beta\gamma(\beta\gamma\delta-\sqrt{\Delta})+(\beta\gamma(\gamma-\delta)-\sqrt{\Delta})\omega+\gamma\omega^2}{2\alpha\beta\gamma\omega}}\right)}\times\sqrt{4-(e^{-\frac{h^\alpha c}{2\alpha\beta\gamma}})^2-2e^{-\frac{h^\alpha c}{2\alpha\beta\gamma}}e^{-\frac{h^\alpha d}{2\alpha\omega}}-(e^{-\frac{h^\alpha d}{2\alpha\omega}})^2},$$

$$\zeta_1=\frac{\beta\gamma e^{-\frac{h^\alpha c}{2\alpha\beta\gamma}}\left(e^{\frac{h^\alpha c}{2\alpha\beta\gamma}}-e^{\frac{h^\alpha d}{2\alpha\omega}}\right)}{2\left(-1+e^{\frac{h^\alpha d}{2\alpha\omega}}\right)},$$

$$\zeta_2=\frac{\beta\gamma\sqrt{4-(e^{-\frac{h^\alpha c}{2\alpha\beta\gamma}})^2-2e^{-\frac{h^\alpha c}{2\alpha\beta\gamma}}e^{-\frac{h^\alpha d}{2\alpha\omega}}-(e^{-\frac{h^\alpha d}{2\alpha\omega}})^2}}{2-2e^{-\frac{h^\alpha d}{2\alpha\omega}}}.$$

Moreover, for σ sufficently close to $\overline{\sigma}$, we can express any vector $V\in\mathbf{R}^2$ as $V=zq+\bar{z}\bar{q}$, where z is a complex number. Accordingly, for sufficently small $|\sigma|$ (near $\overline{\sigma}$), the system (13) can be expressed in the following form:

$$z\mapsto\lambda_1z+g(z,\bar{z},\sigma),$$

where $\lambda_1(\sigma)=(1+\psi(\sigma))e^{i\theta(\sigma)}$ with $\psi(\sigma)$ is a smooth function satisfying $\psi(\overline{q})=0$, g is a complex-valued smooth function of $z,\bar{z},\sigma$, whose Taylor expression with respect to $(z,\bar{z})$ contains quadratic and higher order terms

$$g(z,\bar{z},\sigma)=\sum_{k+l\geq 2}\frac{1}{k!l!}g_{k,l}(\sigma)z^k\bar{z}^l,\quad g_{kl}\in\mathbf{C},\quad k,l=0,1,2,\ldots$$

By using multilinear functions, we can determine the Taylor coefficients g_{kl} through the following formulas:

$$\begin{aligned}&g_{20}(\overline{\sigma})=<p,B(q,q)>,\quad g_{11}(\overline{\sigma})=<p,B(q,\overline{q})>,\\&g_{02}(\overline{\sigma})=<p,B(\overline{q},\overline{q})>,\quad g_{21}(\overline{\sigma})=<p,C(q,q,\overline{q})>.\end{aligned}\tag{14}$$

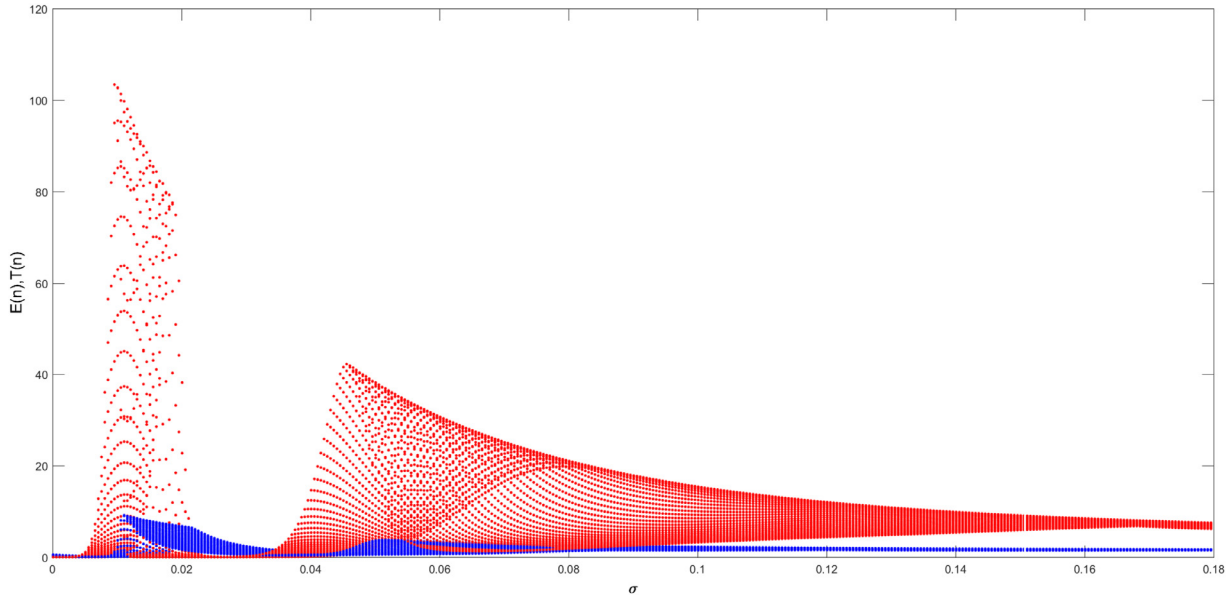

Fig. 3. Bifurcation diagram for the model (9) according to the parameter σ where $\alpha = 0.90$. Other parameter values and initial condition are the same as in Fig. 2.

Table 1
Parameter values used for numerical analysis.

Dimensional Parameters	Biological Meanings	Dimensional Values	Dimensionless Parameters	Dimensionless Values
s	Constant source rate of ECs	1.3×10^4 cells day^{-1}	σ	0.1181 [24,25]
α_1	Immune response to the TCs	$10^{-9}, 10^{-7}$ (day cells)$^{-1}$	ω	0.04 [25]
d	Natural death rate of ECs	0.0412 day^{-1}	δ	0.3743 [24,25]
a	Intrinsic tumor growth rate	0.18 day^{-1}	γ	1.636 [24,25]
b	b^{-1}Carrying capacity of TCs	2×10^{-9} cells^{-1}	β^{-1}	0.002 [24,25]

Hence, the coefficint $k(\overline{\sigma})$, which determines direction of Neimark-Sacker bifurcation, can be calculated via the formula

$$k(\overline{\sigma}) = Re\left(\frac{e^{-i\theta(\overline{\sigma})}g_{21}}{2}\right) - Re\left(\frac{(1-2e^{i\theta(\overline{\sigma})})e^{-2i\theta(\overline{\sigma})}}{2(1-e^{i\theta(\overline{\sigma})})}g_{20}g_{11}\right) - \frac{1}{2}|g_{11}|^2 - \frac{1}{4}|g_{02}|^2, \quad (15)$$

where $e^{i\theta(\overline{\sigma})} = \lambda_1(\overline{\sigma})$.

Using the above arguments and the theorems in [32–34], we achieve the following result.

Theorem 5. *System (9) undergoes a Neimark-Sacker bifurcation at the coexistence equilibrium point E_1 if $\sigma = \overline{\sigma}$ and $k(\overline{\sigma}) \neq 0$. Moreover, if $k(\overline{\sigma}) < 0$ (respectively $k(\overline{\sigma}) > 0$), there exists a unique closed invariant curve bifurcate from E_1 is asymptotically stable (respectively unstable).*

3.4. Numerical results

In this section, we present numerical simulations which verify the theoretical analysis described above. The bifurcation diagram of the system (9) given in Fig. 3. For the parameter values given in Table 1, the system undergoes a Neimark-Sacker bifurcation about the coexistence equilibrium point $E_1 = (1.60922, 8.18465)$ for $\sigma = \overline{\sigma} = 0.0754947$ which shows correctness of Theorem 5. For $\sigma = \overline{\sigma}$, we have complex conjugate eigenvalues $\lambda_{1,2} = 0.99486 \pm 0.101259i$ with modulus $|\lambda_{1,2}| = 1$ and the transversality condition $\frac{d|\lambda_{1,2}(\sigma)|}{d\sigma}\Big|_{\sigma=\overline{\sigma}} = -0.0679214 \neq 0$ is satisfied. Afterwards, the Taylor coefficients can be calculated as $g_{20} = -0.06308 + 0.0825956i$, $g_{02} = -0.0833597 + 0.0865614i$, $g_{11} = 0.0406717 - 0.000501182i$, $g_{21} = 0.00353831 + 0.00571028i$ and therefore the critical value (15) for Neimark-Sacker bifurcation is $k(\overline{\sigma}) = -0.00720469 < 0$. Hence, we conclude that the Neimark-Sacker bifurcation is supercritical (Fig. 4d, Fig. 5c).

4. Results and discussion

In this paper, we have considered two fractional order tumor model that is given as system of fractional differential Eqs. (5) and (6) which have Caputo and conformable fractional derivative respectively. We show that coexistence equilibrium point of the model (5) is always asymptotically stable and Hopf bifurcation does not occur at the coexitence equilibrium point under the condition $\sigma < \gamma\delta$. Then, the conformable fractional order form of the model that is given as (6) is discretized by using piecewise constant approximation and we obtain two-dimensional discrete dynamical system (9). Thus, the fractional order parameter α is included as a new parameter into the system of difference equations.

Bifurcation analysis show that there is no stationary or flip bifurcation for the discrete system (9) because of that the conditions $1 + p_1 + p_0 > 0$ and $1 - p_1 + p_0 > 0$ are always hold. We also prove that the discrete system (9) undergoes a Neimark-Sacker bifurcation at the equilibrium point E_1 depending on the parameter σ which represents the normal rate of the flow of adult ECs into the tumor cite. From the biological point of view, the value of σ can be increased by the therapy of bone marrow transplantation(BMT). Although the therapy of BMT in cancer treatment is relatively new compared to standard chemotherapeutic and radiotherapy regimens, it is explored and applied widely in cancer treatment [39,40].

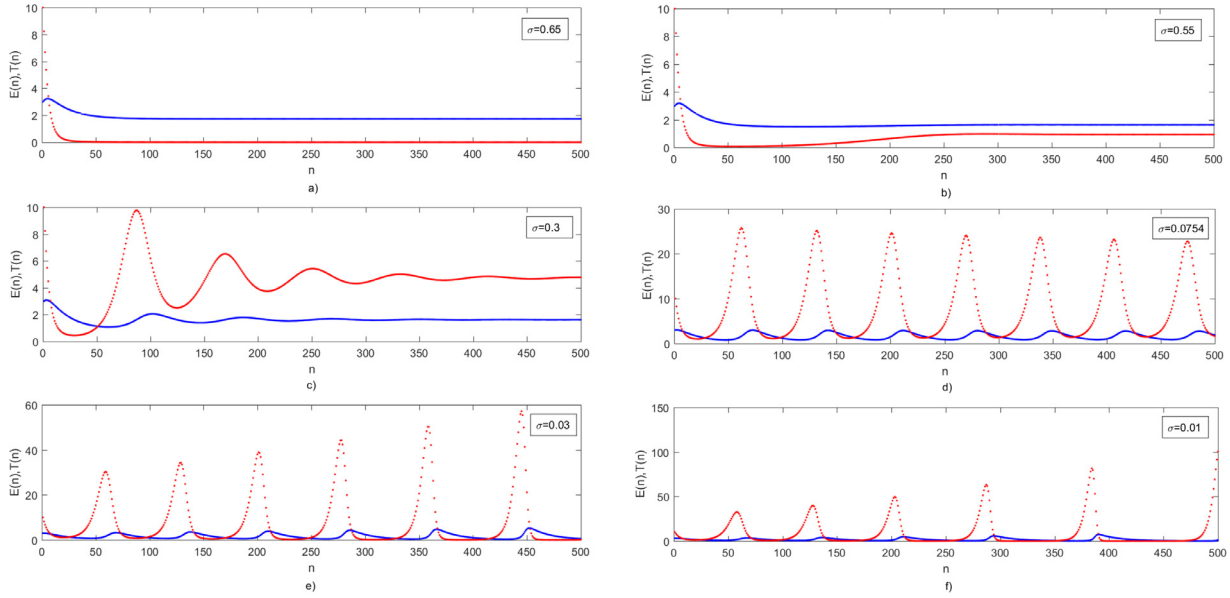

Fig. 4. Dynamical behavior of the system (9) with varying the parameter σ. Initial condition and other parameters are the same as in Fig. 2 where ECs and TCs represented by blue and red curves respectively. (For interpretation of the references to colour in this figure legend, the reader is referred to the web version of this article.)

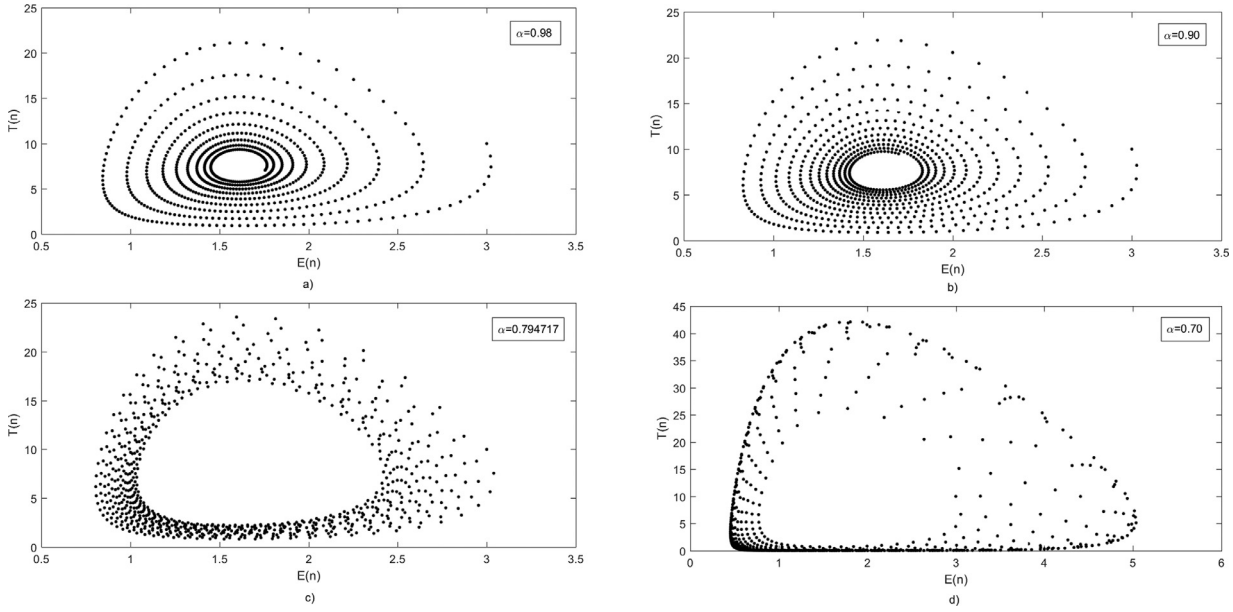

Fig. 5. Phase diagrams of the system (6) depending on the fractional order parameter α.

The importance of Neimark-Sacker bifurcation in this study is that, at the bifurcation point stable periodic solutions occurs around the positive equilibrium point. This mathematical result has been observed clinically and is known as Jeff's Phenomenon [41]. It means that tumor cells exhibit oscillatory behavior around the coexistence equilibrium point without any treatment.

In order to explore the effects of variation of the constant source rate of ECs, we change σ and keep other parameters fixed. From Theorem 5, the critical Neimark-Sacker bifurcation value is obtained as $\sigma = \overline{\sigma} \approx 0.0754$ for the coexistence equilibrium point E_1 (Fig. 3, Fig. 4d). As σ decreases, both equilibrium points remains unstable and the system exhibits oscillatory behaviour with higher amplitude of oscillations (Fig. 4e and f). For $\sigma = 0.3 > \overline{\sigma}$, both ECs and TCs approaches to the coexistence equilibrium point $E_1 \approx (1.62, 4.72)$ in a damped oscillatory mode (Fig. 4c) and namely the state of the dormant tumor is obtained [24,25]. For $\sigma = 0.55$, the system loses its oscillatory behavior and the TCs extinct for a while, then ECs and TCs approaches to the coexistence equilibrium point $E_1 \approx (1.63, 0.93)$ (Fig. 4b). This attitude corresponds to the state of a "returning tumor"[35]. As σ increases and passing the value of $\gamma\delta \approx 0.612$, the ECs succeeded in eradicating the TCs completely and the patient is ultimately cured (Fig. 4a).

In addition, we vary the parameter α and keep other parameters fixed in order to explore the effects of fractional order parameter. Using the equality (10), the critical Neimark-Sacker bifurcation value is obtained as $\alpha = 0.794117$. Fig. 5 shows that the stable behaviour of the system is destabilized when fractional order α is decreasing.

Lyapunov exponents is a useful tool which quantify the chaotic behaviour of discrete system and the sensitive dependance on initial conditions. Finally, we compute maximum Lyapunov exponents of system (9) and explore the dependance of these Lyapunov

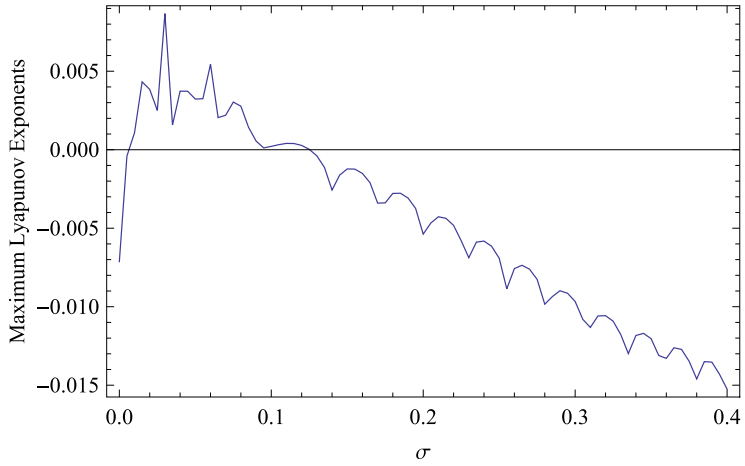

Fig. 6. Maximum Lyapunov exponents of system (9) corresponding to the parameter σ.

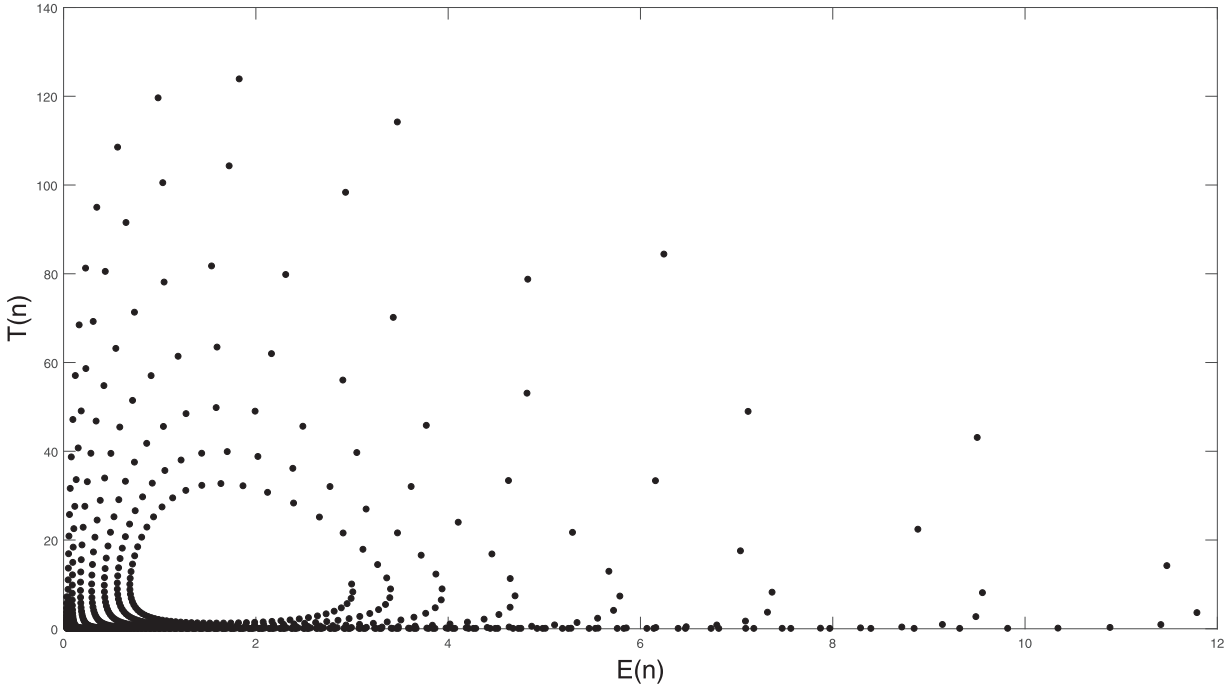

Fig. 7. Chaotic attroctor of the system (9) where parameter taken as in Fig. 4,(f).

exponents on parameter σ which describes the constant source rate of immune cells. We vary the parameter σ in interval [0, 0.4] and keep other parameters fixed as in Table 1. As we saw in Fig. 6, when σ gets smaller than $\sigma = 0.075445$, we obtained positive Lyapunov exponents and the system (9) tends to exhibit chaotic behaviour (See also Fig. 3, Fig. 4f, Fig. 7).

It is well known that fractional order dynamical systems with Caputo or Riemann Liouville sense are more suitable to model tumor-immune system interactions because this derivative involves memory and which is quite favorable to work on biological processes. However, Caputo and Riemann-Liouville also have a big problem that, their kernel although nonlocal but is singular. This weakness has effect when modeling real world problems [42]. Conformable fractional derivative has been put forward to overcome difficulties emerging Caputo fractional derivative in applications. This derivative is not perhaps a fractional derivative but has a fractional order and is a natural extension of classical derivative.

In this paper, we consider two fractional order models with Caputo and conformable sense for the tumor-immune system interactions and compare the obtained results. Numerical simulations show that both of the models exhibit different dynamic behaviors. Discrete version of the conformable fractional order model (9) describes a wider class of tumor growth dynamics then of the Caputo fractional order model (4) such as Neimark-Sacker bifurcation and chaos. Because the tumor growth before therapy is chaotic [43], it may be advantageous to use the model (9) instead of the model (4) for the tumor-immune interaction.

Acknowledgements

This work was supported by Research Fund of the Erciyes University. Project Number: FDK-2018-8119.

References

[1] Tarasov VE. Fractional vector calculus and fractional maxwell's equations. Ann Phys (N Y) 2008;323(11):2756–78. doi:10.1016/j.aop.2008.04.005.
[2] Laskin N. Fractional schrdinger equation. Phys Rev E 2002;66:056108. doi:10.1103/PhysRevE.66.056108.

[3] Yuste SB, Acedo L, Linderberg K. Reaction front in an a+b→ c reaction-subdiffusion process. Phys Rev E 2004;69:036126. doi:10.1103/PhysRevE.69.036126.
[4] Chen WC. Nonlinear dynamics and chaos in a fractional order financial system. Chaos, Solitons Fractals 2008;36(5):1305–14. doi:10.1016/j.chaos.2006.07.051.
[5] Ferdi Y. Some applications of fractional order calculus to design digital filters for biomedical signal processing. J Mech Med Biol 2012;12(2):124008. doi:10.1142/S0219519412400088.
[6] Spanos PD, Malara G. Random vibrations of nonlinear continua endowed with fractional derivative elements. Procedia Eng 2017;199:18–27. doi:10.1016/j.proeng.2017.09.144.
[7] Pinto CMA, Machado JT. Fractional model for malaria transmission under control strategies. Comput Math Appl 2013;66(5):908–16. doi:10.1016/j.camwa.2012.11.017.
[8] Bolton L, Cloot AH, Schoombie SW, Slabbert JP. A proposed fractional-order gompertz model and its application to tumour growth data. Math Med Biol 2015;32(2):187–207. doi:10.1093/imammb/dqt024.
[9] Baleanu D, Jajarmi A, Bonyah E, Hajipour M. New aspects of poor nutrition in the life cycle within the fractional calculus. Adv Differ Eqs 2018;2018:230. doi:10.1186/s13662-018-1684-x.
[10] Podlubny I. Fractional differential equations. Academic Press New York; 1999.
[11] Petras I. Fractional-order nonlinear systems: modeling, analysis and simulation. Springer Berlin; 2011.
[12] Baisad K, Moonchai S. Analysis of stability and hopf bifurcation in a fractional gauss-type predator-prey model with allee effect and holling type-III functional response. Adv Differ Eqs 2018;2018:82. doi:10.1186/s13662-018-1535-9.
[13] Khalil R, Horani MA, Yousef A, Sababheh M. A new definition of fractional derivative. J Comput Appl Math 2014;264:65–70. doi:10.1016/j.cam.2014.01.002.
[14] Abdeljawad T. On conformable fractional calculus. J Comput Appl Math 2015;279:57–66. doi:10.1016/j.cam.2014.10.016.
[15] Chung WS. Fractional newton mechanics with conformable fractional derivative. J Comput Appl Math 2015;290:150–8. doi:10.1016/j.cam.2015.04.049.
[16] Rosales JJ, Godinez FA, Banda V, Valencia GH. Analysis of the drude model in view of the conformable derivative. Optik 2019;178:1010–15. doi:10.1016/j.ijleo.2018.10.079.
[17] Kartal S, Gurcan F. Discretization of conformable fractional differential equations by a piecewise constant approximation. Int J Comput Math 2018. doi:10.1080/00207160.2018.1536782.
[18] Atangana A. A novel model for the lassa hemorrhagic fever: deathly disease for pregnant woman. Neural Comput Applic 2015;26:1895–903.
[19] Perez JES, Gomez-Aguilar JF, Baleanu D, Tchier F. Chaotic attractors with fractional conformable derivatives in the liouville-caputo sense and its dynamical behaviours. Entropy 2018;20(5):384. doi:10.3390/e20050384.
[20] Jafari H, Daftardar-Gejji V. Solving a system of nonlinear fractional differential equations using adomian decomposition. J Math Anal Appl 2006;196:644–51.
[21] Ameen I, Novati P. The solution of fractional order epidemic model by implicit adams methods. Appl Math Model 2017;43:78–84. doi:10.1016/j.apm.2016.10.054.
[22] Momani S, Odibat Z. Numerical approch to differential equations of fractional order. J Comput Appl Math 2007;207:96–110. doi:10.1016/j.cam.2006.07.015.
[23] Ibis B, Bayram M. Numerical comparison of methods for solving fractional differential algebraic equations (FDAEs). Computers and Mathematics with Applications 2011;62(8):3270–8. doi:10.1016/j.camwa.2011.08.043.
[24] Kuznetsov VA, Makalkin IA, Taylor MA, Perelson S. Nonlinear dynamics of immunogenic tumors: parameter estimation and global bifurcation analysis. Bull Math Biol 1994;56(2):295–321. doi:10.1016/S0092-8240(05)80260-5.
[25] Galach M. Dynamics of the tumor-immune system competition-the effect of the time delay. Int J Math Comput Sci 2003;13(3):395–406.
[26] Rihan FA, Hashish A, Al-Maskari F, Sheek-Hussin M, Ahmed E, Riaz MB, Yafia R. Dynamics of tumor-immune system with fractional order. J Tumor Res 2016;2(109).
[27] El-Raheem ZF, Salman SM. On a discretization process of fractional-order logistic differential equation. J Egypt Math Soc 2014;22:407–12. doi:10.1016/j.joems.2013.09.001.
[28] El-sayed AMA, El-Raheem ZF, Salman SM. Disretization of forced duffing system with fractional-order damping. Adv Differ Eqs 2014. doi:10.1186/1687-1847-2014-66.
[29] Agarwal RP, El-sayed AMA, Salman SM. Fractional-order chua's system: discretization, bifurcation and chaos. Adv Differ Equs 2013. doi:10.1186/1687-1847-2013-320.
[30] Gopalsamy K, Liu P. Persistence and global stability in a population model. J Math Anal Appl 1998;224:59–80. doi:10.1006/jmaa.1998.5984.
[31] Murray JD. Mathematical biology. Springer New York; 1993.
[32] Kuznetsov VA. Elements of applied bifurcation theory. Springer New York; 1998.
[33] Guckenheimer J, Holmes P. Nonlinear oscillations, dynamical systems and bifurcations of vector fields. Springer New York; 1983.
[34] Wiggins S. Introduction to applied nonlinear dynamical systems and chaos. Springer New York; 2003.
[35] Kirscner D, Panetta JC. Modeling immunotherapy of the tumor-immune interaction. J Math Biol 1998;37(3):235–52. doi:10.1007/s002850050127.
[36] Diethelm K. An algorithm for the numerical solution of differential equations of fractional order. Electron Trans Numer Anal 1997;5:1–6.
[37] Diethelm K, Ford NJ, Freed AD. A predictor-corrector approch for the numerical solution of fractional differential equations. Nonlinear Dyn 2002;29:3–22. doi:10.1023/A:1016592219341.
[38] Garrappa R. On linear stability of predictor-corrector algorithms for fractional differential equations. Int J Comput Math 2010;87(10):2281–90. doi:10.1080/00207160802624331.
[39] Benowitz S. Bone marrow experts are still debating the value of purging. J Natl Cancer I 2000;92(3). 190a-192. doi: 10.1093/jnci/92.3.190A.
[40] Rosenfeld MR, Pruitt A. Neurologic complications of bone marrow, stem cell, and organ transplantation in patients with cancer. Semin Oncol 2006;33(3):352–61. doi:10.1053/j.seminoncol.2006.03.003.
[41] Thomlinson R. Measurement and management of carcinoma of the breast. Clin Radiol 1982;33:481–92.
[42] Atangana A, Koca I. Chaos in a simple nonlinear system with atangana-baleanu derivatives with fractional order. Chaos Soliton Fractal 2016;89:447–54.
[43] Moghtadaei M, Golpayegani MRH, Malekzadeh R. Periodic and chaotic dynamics in a map-based model of tumor–immune interaction. J Theor Biol 2013;334(7):130–40.